

# 1 Ridge regression baseline model outperforms deep learning 2 method for cancer genetic dependency prediction

3  
4 Daniel Chang<sup>1</sup> and Xiang Zhang<sup>1</sup>

5  
6 <sup>1</sup>Department of Computer Science and Engineering, University of Minnesota, Minneapolis, MN  
7 55455, USA

## 8 9 Abstract

10 Accurately predicting genetic or other cellular vulnerabilities of unscreened, or difficult to  
11 screen, cancer samples will allow vast advancements in precision oncology. We re-analyzed a  
12 recently published deep learning method for predicting cancer genetic dependencies from their  
13 omics profiles. After implementing a ridge regression baseline model with an alternative,  
14 simplified problem setup, we achieved a model that outperforms the original deep learning  
15 method. Our study demonstrates the importance of problem formulation in machine learning  
16 applications and underscores the need for rigorous comparisons with baseline approaches.

## 17 18 Main

19 Precision oncology methods rely on the ability to accurately translate molecular measurements of  
20 tumors to insights about their genetic dependencies or other cellular vulnerabilities, ultimately  
21 dictating targeted therapeutics. Through genome-wide CRISPR-Cas9 knockout screens, the  
22 Cancer Dependency Map(1–5) (DepMap) has characterized the genetic dependency profiles of  
23 over 1000 cancer cell lines (CCLs). Using the DepMap 2018Q2 release, Chiu *et al.* recently  
24 developed DeepDEP, a deep learning method for predicting genetic dependency profiles of CCLs  
25 given their multi-omics(6). DeepDEP was reported to vastly outperform baseline conventional  
26 machine learning models. However, we argue here that this result can be attributed to aspects of  
27 its problem formulation.

28  
29 Notably, DeepDEP does not jointly predict the entire genetic dependency profile of an input  
30 CCL at once. Instead, the model takes as input both multi-omics of a CCL and a functional  
31 fingerprint of a single gene dependency of interest (DepOI, as abbreviated by Chiu *et al.*), and  
32 outputs the predicted score of that specific gene DepOI for that CCL (Fig. 1A). Functional  
33 fingerprints were defined as binary vectors encoding a gene’s involvement in 3115 chemical and  
34 genetic perturbations (CGPs) from MSigDB v6.2(7), potentially facilitating the model to learn  
35 relationships between genes with functional similarities.

36  
37 We recognized that this problem formulation, while likely beneficial for embedding prior  
38 knowledge about a gene DepOI’s function in a deep learning context, could be problematic for  
39 simpler baseline models as it requires a model to learn highly non-linear relationships between

input omics features and dependency scores. Because this formulation requires a singular model to predict the score of any gene DepOI (given its functional fingerprint representation), the model is unable to directly relate input omics features to dependency scores. Instead, an optimal model must first generate intermediate representations composed of both a CCL’s input omics features and the DepOI’s fingerprint vector. Because Chiu *et al.* evaluated baseline model performances using this setup, we were skeptical about the degree by which DeepDEP truly outperforms baseline methods.

To evaluate this, we implemented a ridge regression baseline model using a simplified problem formulation (Fig. 1B). Instead of outputting a single gene dependency score for a CCL and gene DepOI combination, our baseline jointly outputs predictions of an input CCL's genetic dependency profile across 1298 cancer relevant genes (defined by Chiu *et al.*), the same gene DepOI set on which DeepDEP was trained and evaluated.

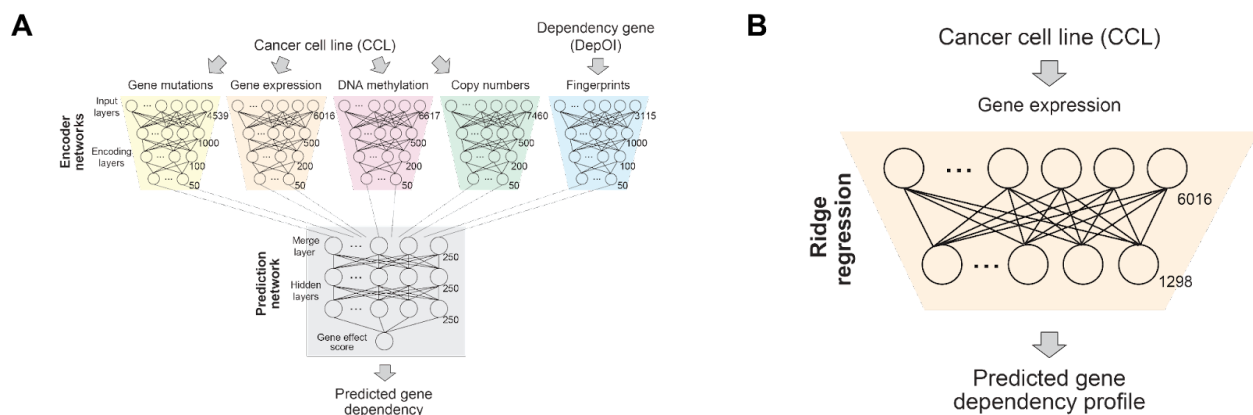
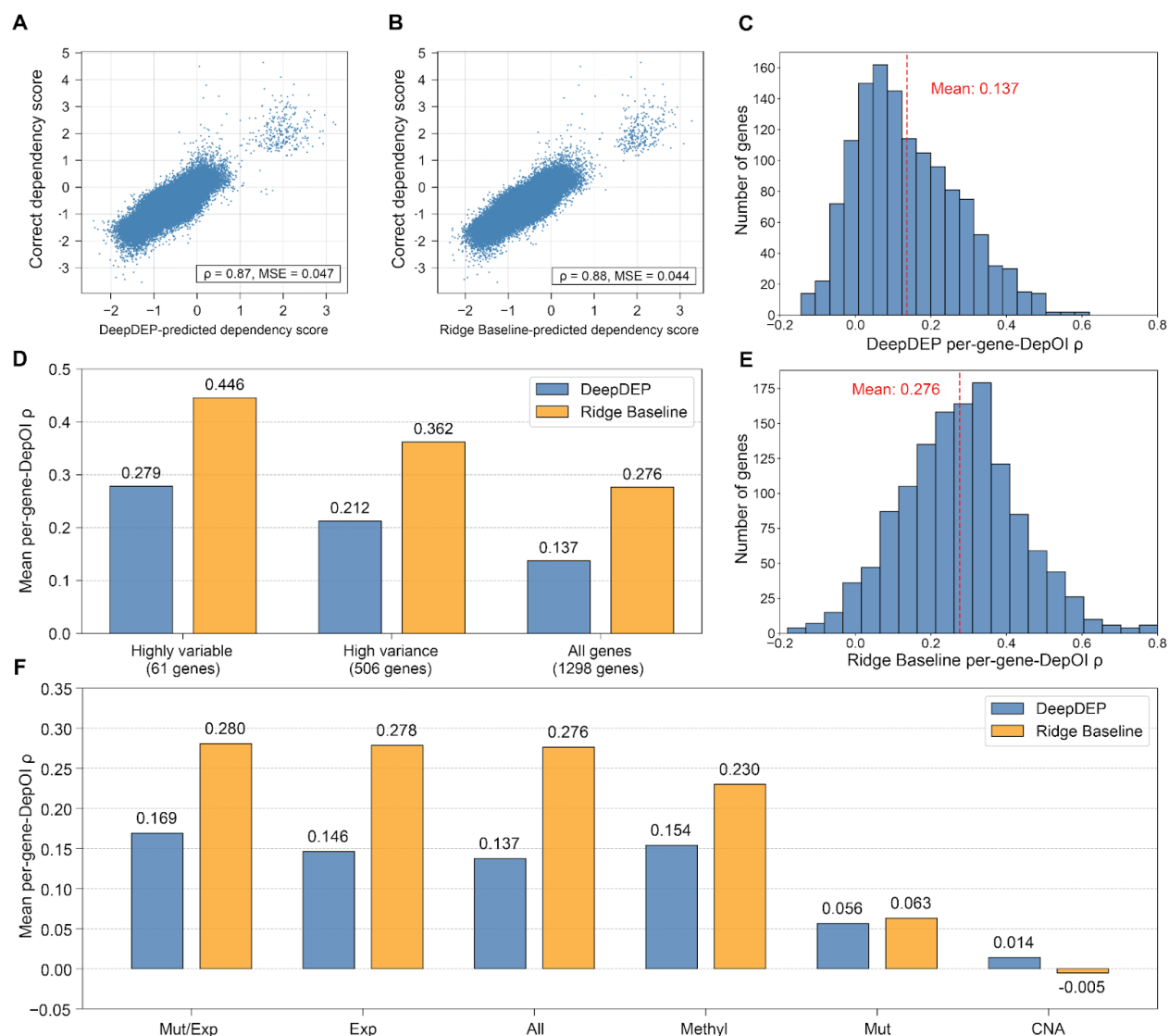


**Fig. 1. Comparison of DeepDEP and baseline setups.** (A) DeepDEP architecture (taken directly from Chiu *et al.*). DeepDEP takes as input a CCL's DNA mutation, gene expression, DNA methylation, and copy number alteration profiles. In addition, a functional fingerprint of a gene dependency of interest (DepOI) is supplied. Dimensionality of each input is displayed. DeepDEP performs dimensionality reduction using an autoencoder pretrained on 8238 TCGA tumors. The model then merges the dimensionality-reduced data into a prediction network to predict the score of the gene DepOI (corresponding to the input functional fingerprint) for a given CCL. (B) Baseline model setup. A multioutput ridge regression model takes as input omics data (in this illustration, just gene expression) from a CCL, and predicts its genetic dependency profile across 1298 cancer relevant gene DepOIs, as defined by Chiu *et al.*

We compared 10-fold cross validation results of DeepDEP and a ridge regression baseline using the aforementioned simplified setup. The ridge regression baseline here uses all input omics features, but no functional fingerprints. Across 278 CCLs and 1298 gene DepOIs, DeepDEP and the ridge regression baseline achieved similar predictive performances (DeepDEP: Fig. 2A, Pearson correlation coefficient  $\rho = 0.87$ ; ridge regression baseline: Fig. 2B,  $\rho = 0.88$ ). However, because of the existence of pan-essential genes, for which dependency score predictions are mostly constant across CCLs and thus easy to predict, analyzing correlation results across all

genes likely yields an overly-optimistic estimate of model performances. Thus, we next evaluated the results by computing correlations per-gene-DepOI. DeepDEP achieved a mean per-gene-DepOI  $\rho$  of 0.137 (Fig. 2C), while the ridge regression baseline achieved a  $\rho$  of 0.276 (Fig. 2E). The ridge regression baseline (with this simplified setup) not only achieved a result higher than that of any baseline machine learning methods evaluated by Chiu *et al.* (not shown here), but also outperformed the full DeepDEP model.



80

81

**Fig. 2. Ridge regression baseline outperforms DeepDEP.** (A and B) Scatterplots of DeepDEP (x-axis, A) and ridge baseline (x-axis, B) predicted dependency scores vs the correct dependency scores (y-axis) across 278 CCLs and 1298 gene DepOIs. 10-fold cross-validation, where CCLs are held out, was used to generate predictions for both models. DeepDEP achieves  $\rho = 0.87$  and mean squared error (MSE) = 0.047. The ridge baseline achieves  $\rho = 0.88$  and MSE = 0.044. (C and E) Histogram of per-gene-DepOI  $\rho$  for DeepDEP and the ridge baseline. DeepDEP achieves a mean  $\rho$  of 0.137, and the ridge baseline achieves a mean  $\rho$  of 0.276. (D) Mean per-gene-DepOI  $\rho$  for (as defined in Chiu *et al.*) highly variable dependency score genes ( $n = 61$ ), high variance dependency score genes ( $n =$

506), and the entire gene set ( $n = 1298$ ). The ridge regression baseline model outperforms DeepDEP on all gene sets. (F) Simplified models trained on subsets of the omics data. Mut = mutation, Exp = gene expression, Methyl = methylation, and CNA = copy number alteration. For all simplified models except that trained on just CNA data, the ridge regression baseline achieves a higher mean per-gene-DepOI  $\rho$  than DeepDEP does.

Chiu *et al.* also analyzed mean per-gene-DepOI  $\rho$  on two subsets of genes that were observed to have high variance dependency scores and thus were likely cancer-relevant genes. The ridge regression baseline model outperformed DeepDEP on both of these gene sets (Fig. 2D).

We next constructed several simplified ridge models using subsets of the omics data types (for example, Fig. 1B depicts an expression-only ridge model), similarly as done in Chiu *et al.* These simplified models were compared with DeepDEP results. In all instances except when using only copy number alteration data, the ridge regression baseline achieves a higher mean per-gene-DepOI  $\rho$  than DeepDEP does (Fig. 2F).

These results demonstrate how machine learning problem formulations dramatically impact the performance of baseline approaches. We show that a problem formulation that is convenient for embedding information into deep learning models may not always be the ideal formulation for baseline approaches. To truly evaluate the degree by which novel methods outperform baselines, it is necessary to rigorously evaluate baselines using different, potentially simpler, problem formulations. Moreover, many of our simplified ridge regression baselines, trained on subsets of the data types (Mut/Exp, Exp, Methyl), outperformed DeepDEP trained on all input genomic features. This demonstrates that the proposed deep learning model was not able to benefit from integrating information from a diverse set of data modalities. We also demonstrate how the use of gene functional fingerprints is not important for achieving an elevated prediction performance over DeepDEP. These results bring into question the strength of the results obtained from downstream analyses using the DeepDEP model, such as the pan-cancer tumor dependency map that Chiu *et al.* generated by applying DeepDEP on TCGA data.

Overall, we demonstrate the importance of conducting rigorous baselines when evaluating the performance of novel methods, and the importance of considering the implications of different machine learning problem formulations.

## Data and code availability

All data was obtained from the Code Ocean compute capsule accompanying Chiu *et al.*, the supplementary tables of Chiu *et al.*, and from the DepMap portal. Machine learning tasks were performed using Scikit-learn v1.2.2(8). All code and data for this analysis can be found at: [https://github.com/danielchang2002/deepdep\\_reanalysis](https://github.com/danielchang2002/deepdep_reanalysis).

## 128 Methods

129 DeepDEP CCL dependency score predictions from 10-fold cross-validation (where CCLs are  
130 held out) were obtained from Supplementary Table S8 of Chiu *et al.* Ground truth gene effect  
131 scores of the 278 CCLs were obtained from the DepMap 2018Q2 release. The DeepDEP 10-fold  
132 cross-validation dependency score predictions were compared with the ground truth in Fig. 2A  
133 and 1C.

134

135 DNA mutation, gene expression, DNA methylation, and copy number alteration data of the 278  
136 CCLs were obtained from the Code Ocean compute capsule accompanying Chiu *et al.*

137 Functional fingerprints were not used in our analysis. Ridge regression  
138 (`sklearn.linear_model.Ridge`) with default parameters was then used to predict an input CCL's  
139 genetic dependency profile across 1298 cancer relevant genes (defined by Chiu *et al.*), the same  
140 gene DepOI set on which DeepDEP was trained and evaluated, given a flattened vector of the  
141 four data types concatenated together for an input CCL. Ridge regression baseline prediction  
142 scores were obtained via 10-fold cross-validation (where CCLs are held out). Notably, the CCL  
143 fold partitioning is not identical to that used to generate DeepDEP cross-validation results in  
144 Supplementary Table S8 of Chiu *et al.*, but generated independently in this analysis  
145 (`sklearn.model_selection.KFold`; `random_state = 42`). Ridge regression baseline 10-fold  
146 cross-validation scores were compared with the ground truth in Fig. 2B and 2E.

147

148 The gene set of 61 “highly variable” genes was obtained by locating genes with dependency  
149 score standard deviations greater than 0.3, as defined by Chiu *et al.* The gene set of 506 “high  
150 variance” genes was obtained using the “Achilles\_high\_variance\_genes.csv” file provided by the  
151 DepMap portal. The 10-fold cross-validation results on these two gene subsets, for both the  
152 Ridge regression baseline and DeepDEP, are detailed in Fig. 2D.

153

154 Results for simplified ridge regression baseline models were obtained using subsets of the CCL  
155 omics data. This was performed identically as before, using 10-fold cross-validation. However,  
156 for DeepDEP, the 10-fold cross-validation prediction scores were only available (in the  
157 supplementary of Chiu *et al.*) for the model using all omics features (i.e. the “All” model), and  
158 not for the simplified models. Thus, in Fig. 2F, simplified DeepDEP model performances were  
159 obtained using data from Supplementary Fig. S5 of Chiu *et al.*, which details per-gene-DepOI p  
160 for simplified models using 10 independent train-test subsampling (i.e., a slightly different  
161 evaluation method than 10-fold cross-validation).

162

## 163 References

- 164 1. R. M. Meyers, J. G. Bryan, J. M. McFarland, B. A. Weir, A. E. Sizemore, H. Xu, N. V. Dharia, P. G.  
165 Montgomery, G. S. Cowley, S. Pantel, A. Goodale, Y. Lee, L. D. Ali, G. Jiang, R. Lubonja, W. F.  
166 Harrington, M. Strickland, T. Wu, D. C. Hawes, V. A. Zhivich, M. R. Wyatt, Z. Kalani, J. J. Chang,  
167 M. Okamoto, K. Stegmaier, T. R. Golub, J. S. Boehm, F. Vazquez, D. E. Root, W. C. Hahn, A.

- 168 Tsherniak, Computational correction of copy number effect improves specificity of CRISPR-Cas9  
169 essentiality screens in cancer cells. *Nat. Genet.* **49**, 1779–1784 (2017).
- 170 2. M. Ghandi, F. W. Huang, J. Jané-Valbuena, G. V. Kryukov, C. C. Lo, E. R. McDonald, J. Barretina,  
171 E. T. Gelfand, C. M. Bielski, H. Li, K. Hu, A. Y. Andreev-Drakhlin, J. Kim, J. M. Hess, B. J. Haas,  
172 F. Aguet, B. A. Weir, M. V. Rothberg, B. R. Paoletta, M. S. Lawrence, R. Akbani, Y. Lu, H. L. Tiv, P.  
173 C. Gokhale, A. de Weck, A. A. Mansour, C. Oh, J. Shih, K. Hadi, Y. Rosen, J. Bistline, K.  
174 Venkatesan, A. Reddy, D. Sonkin, M. Liu, J. Lehar, J. M. Korn, D. A. Porter, M. D. Jones, J. Golji,  
175 G. Caponigro, J. E. Taylor, C. M. Dunning, A. L. Creech, A. C. Warren, J. M. McFarland, M.  
176 Zamanighomi, A. Kauffmann, N. Stransky, M. Imielinski, Y. E. Maruvka, A. D. Cherniack, A.  
177 Tsherniak, F. Vazquez, J. D. Jaffe, A. A. Lane, D. M. Weinstock, C. M. Johannessen, M. P.  
178 Morrissey, F. Stegmeier, R. Schlegel, W. C. Hahn, G. Getz, G. B. Mills, J. S. Boehm, T. R. Golub, L.  
179 A. Garraway, W. R. Sellers, Next-generation characterization of the Cancer Cell Line Encyclopedia.  
180 *Nature*. **569**, 503–508 (2019).
- 181 3. C. Pacini, J. M. Dempster, I. Boyle, E. Gonçalves, H. Najgebauer, E. Karakoc, D. van der Meer, A.  
182 Barthorpe, H. Lightfoot, P. Jaaks, J. M. McFarland, M. J. Garnett, A. Tsherniak, F. Iorio, Integrated  
183 cross-study datasets of genetic dependencies in cancer. *Nat. Commun.* **12**, 1–14 (2021).
- 184 4. J. M. Dempster, J. Rossen, M. Kazachkova, J. Pan, G. Kugener, D. E. Root, A. Tsherniak, Extracting  
185 Biological Insights from the Project Achilles Genome-Scale CRISPR Screens in Cancer Cell Lines.  
186 *bioRxiv* (2019), p. 720243.
- 187 5. J. M. Dempster, I. Boyle, F. Vazquez, D. Root, J. S. Boehm, W. C. Hahn, A. Tsherniak, J. M.  
188 McFarland, Chronos: a CRISPR cell population dynamics model. *bioRxiv* (2021), p.  
189 2021.02.25.432728.
- 190 6. Y.-C. Chiu, S. Zheng, L.-J. Wang, B. S. Iskara, M. K. Rao, P. J. Houghton, Y. Huang, Y. Chen,  
191 Predicting and characterizing a cancer dependency map of tumors with deep learning. *Science*  
192 *Advances* (2021), doi:10.1126/sciadv.abh1275.
- 193 7. A. Liberzon, A. Subramanian, R. Pinchback, H. Thorvaldsdóttir, P. Tamayo, J. P. Mesirov, Molecular  
194 signatures database (MSigDB) 3.0. *Bioinformatics*. **27**, 1739–1740 (2011).
- 195 8. Pedregosa, Varoquaux, Gramfort, Scikit-learn: Machine learning in Python. *the Journal of machine*  
196 (available at  
197 <https://www.jmlr.org/papers/volume12/pedregosa11a/pedregosa11a.pdf?ref=https://githubhelp.com>).